



Simultaneous estimation of GPS P1-P2 differential code biases using low earth orbit satellites data from two different orbit heights

Mingming Liu^{1,2} · Yunbin Yuan¹ · Xingliang Huo¹ · Min Li¹ · Yanju Chai¹

Received: 15 February 2020 / Accepted: 4 November 2020 / Published online: 27 November 2020
© Springer-Verlag GmbH Germany, part of Springer Nature 2020

Abstract

Global navigation satellite system (GNSS) differential code bias (DCB) is a significant error source in ionosphere modeling that uses GNSS observation data. Given that the orbit altitudes of low earth orbit (LEO) satellites are above the F layer of ionosphere, ionized electrons come from the upper ionosphere or plasmasphere, so observations suffer from small signal delays. DCBs can be estimated using LEO data instead of that from ground stations. In most studies, LEO-based DCB estimation employs onboard data from either a single LEO or from two that are at the same orbit height. In our study, we applied four LEO satellites data from two different orbit heights to estimate GPS satellite DCBs, receiver DCBs and LEO-based vertical total electron content (VTEC) parameters simultaneously. Before DCB estimation, a data preprocessing strategy suitable for LEO onboard data was applied to obtain clear pseudorange data. We developed a processing method for the upper ionosphere using LEO onboard data from different orbit heights, by introducing LEO-based VTEC models in advance to remove its effects; two introduced VTEC models were derived from modeling results using paired data from the same orbital height, respectively. We draw some conclusions as follows. For the LEO satellites at different orbit heights, the more the number of LEO satellites involved, the more stable estimation results achieved. We also noted that the GPS satellite DCBs stability and accuracy with established LEO-based VTEC models, using multi-LEOs data from different orbit heights, were better than the achievable results using onboard data from the same orbital height or using single LEO satellite schemes. Compared with the estimation results of single LEO solutions, the monthly stabilities and accuracies for multi-LEOs solutions from different orbit heights are improved by 25–35% approximately. Among all the tested schemes, superior stability derived from simultaneous estimation using four LEO data at different orbit heights is 0.064 ns; the optimal accuracies for DCB estimation for different GPS satellites are the scheme GRACE-A and JASON-2 (two LEOs) of 0.146 ns, approximately, compared with Center of Orbit Determination of Europe products, respectively. The stability and accuracy of LEO-based DCB estimations were approximately similar to those achieved using ground solutions.

Keywords Low earth orbit satellite (LEO) · Onboard GNSS/GPS data · GPS satellite differential code bias (DCB) · Onboard receiver differential code biases (DCB) · Different orbit heights · LEO-based vertical total electron content (VTEC) · Stability and accuracy

1 Introduction

Differential code biases (DCBs) physically denote a time delay caused by the dual-frequency signal travel through

satellite or receiver. DCBs should be calibrated for the navigation, pseudorange-based positioning and timing, and it is also a significant error source in ionosphere modeling (Zhang et al. 2012; Montenbruck and Hauschild 2013; Wang et al. 2015). At present, there are two main ways to compute inter-frequency DCBs according to the differences of ionosphere modeling: DCBs are estimated either simultaneously with global or local ionospheric model (Schaer 1999, 2012; Krankowski et al. 2009; Hernández-Pajares et al. 2011), (such as the Center of Orbit Determination of Europe (CODE), Schaer 1999), or by introducing a priori ionosphere model to remove its influences (such as the Ger-

✉ Yunbin Yuan
yybgps@asch.whigg.ac.cn

¹ State Key Laboratory of Geodesy and Earth's Dynamics, Innovation Academy for Precision Measurement Science and Technology, Chinese Academy of Sciences, Wuhan 430077, China

² University of Chinese Academy of Sciences, Beijing 100049, China

man Aerospace Center (DLR), Montenbruck et al. 2014). Another way is that the methodology developed by the Chinese Academy of Science (CAS) which locally models the vertical total electron content (VTEC) above each station of the network (Li et al. 2012; Wang et al. 2015).

Most DCB product centers extremely depend on the amount of observation data—that is, the number of ground stations and their distribution, receiver types, and data quality affects all the estimated DCB precision. The CODE needs more than two hundred ground stations to support their solutions (Schaer 1999), and the CAS analysis center calculates DCBs using 180 ground stations. Moreover, satellite DCB real-time estimation and its accuracy also require numerous ground stations and high-quality data. Approaches based on ground observations are more sensitive to ionospheric variation. Given that the orbit altitudes of LEO satellites are above the F layer of the ionosphere, ionized electrons come from the upper ionosphere, or plasmasphere, which is less variable in both spatial and temporal domains, so observations suffer from smaller signal delays. Also, since LEO satellites are moving very rapidly—at 7–8 km/s—they can be seen as moving space-based stations, and a smaller number of satellites can be needed to achieve the similar results as ground-based observations; the onboard receiver types and data quality are uniform and stable. These advantages overcome the lack of ground stations, and can provide a different method or data source for estimating navigation satellite DCBs. In fact, BDS-3 also hopes to make the best use of fewer monitoring stations outside China to achieve its routine operation control, such as calculations of time group delay parameters (Yuan et al. 2019; Yang et al. 2020). The LEO satellites participating in DCB estimation play a role of navigation augmentation, which is the essential application function of LEO satellites for basic positioning, navigation and timing (PNT) services (Zhang and Ma 2019).

This LEO-based DCB estimation method has been studied recently. Lin et al. (2014) and Zhong et al. (2015b) considered the GPS satellite and onboard receiver DCB as estimated parameters. Wautelet et al. (2017) simultaneously estimated GPS satellite DCBs, Jason-2 receiver DCBs and VTEC derived from signal propagation, using a least-square adjustment. Meanwhile, many studies only estimate plasmasphere and receiver DCB parameters, using GPS satellite DCBs (Zhang and Tang 2014; Zakharenkova and Cherniak 2015; Zhong et al. 2016). Zhou et al. (2019) estimated GPS DCBs based on uncombined precise point positioning (PPP) with LEO onboard data. Li et al. (2017a) and Li et al. (2019) estimated and analyzed GPS and BDS DCBs based on onboard observations from the FY-3C satellite. Li et al. (2019) estimated navigation satellite DCBs using the FY-3C and FY-3D satellites simultaneously, while others have used just one LEO satellite at a time. Zhong et al. (2015b) took LEO-based VTEC as epoch parameters during DCB

estimation from different heights data. In current most studies, LEO-based DCB estimations employ onboard data from either single or two LEO satellites that are at the same orbit height. In our study, we used four LEO satellites, distributed at two different orbit planes, to develop an ionosphere processing method for onboard data at different orbit heights; in this, we introduced LEO-based VTEC models in advance to remove their effects. Here, two introduced plasmasphere VTEC models were derived from respective modeling results using two paired LEOs data at the same orbit height.

This paper is organized as follows. We firstly depict the preprocessing strategies applied to the LEO onboard data, and illustrate the model and strategies used to estimate satellite DCBs together with the plasmasphere parameters. Next, we show the results of GPS satellite DCBs, onboard receiver DCBs, and the LEO-based VTEC simultaneously estimated using onboard data from four LEO satellites one-by-one, including the GRACE-A and -B and JASON-2 and -3 satellites, to test the reliability of the estimation strategy. Then, we estimated the satellite DCBs and plasmasphere VTEC based on two paired LEOs data at their respective orbit heights and obtained two related plasmasphere VTEC models. The onboard data from four LEO satellites, distributed at two different orbital planes, were processed by introducing two LEO-based VTEC models obtained from the previous step to estimate the satellite and receiver DCBs. Finally, we are able to draw some conclusions in relation to DCB estimation.

2 Methodology and strategies for DCB estimation

DCBs were calculated using LEO space-borne data from satellites orbit planes at both the same and different orbit heights. The DCBs in this paper denote differential P1-P2 code biases. This section elaborates on the models and methods used for satellite DCB estimation, also including data preprocessing, the plasmasphere delay model, and accuracy evaluation. We have also illustrated the differences between our estimation strategies and those of other studies in this section.

2.1 Model and method

Similar to CODE and CAS analysis centers, DCB values (P1-P2) for GPS satellites and onboard receivers are estimated as constant values daily and simultaneously with topside ionosphere or plasmasphere VTEC parameters. The geometry-free (GF) combination observation estimation method has a simpler calculation process and does not need outlier information, such as satellite orbits, clock error information, and so on. Therefore, we employ GF combinations of pseudorange observations to estimate DCB parameters.

Dual-frequency GPS code observations are commonly expressed as shown in Eq. (1), and the GF combination of pseudorange observation is formed and expressed as shown in Eq. (2) (Montenbruck et al. 2014; Wang et al. 2015). Since the orbit height of LEO satellite is above the troposphere, there is no such effect in Eq. (1).

$$\begin{cases} P_{r,1}^s = \rho_r^s + c \cdot (dt_r - dt^s) + \alpha_1 \cdot \text{STEC} + c \cdot (b^{s,1} + b_{r,1}) + \varepsilon_{r,1}^s, \alpha_1 = \frac{40.28}{f_1^2} \\ P_{r,2}^s = \rho_r^s + c \cdot (dt_r - dt^s) + \alpha_2 \cdot \text{STEC} + c \cdot (b^{s,2} + b_{r,2}) + \varepsilon_{r,2}^s, \alpha_2 = \frac{40.28}{f_2^2} \end{cases} \quad (1)$$

$$P_{r,GF}^s = P_{r,1}^s - P_{r,2}^s = \alpha \cdot \text{STEC} + \text{DCB}^s + \text{DCB}_r + \varepsilon_{r,GF}^s, \quad \alpha = 40.28 \cdot \left(\frac{1}{f_1^2} - \frac{1}{f_2^2} \right) \quad (2)$$

where the superscript *s* and *r* represent the GNSS satellite and LEO onboard receiver, and 1, 2 represent frequency number; symbols f_1, f_2 represent the GPS L1 and L2 frequencies; $P_{r,1}^s, P_{r,2}^s$ are the pseudorange observations in meters at GPS L1 and L2 frequencies from GNSS satellite *s* to LEO satellite *r*; ρ_r^s denotes the geometric distance in meters; dt_r, dt^s refer to the receiver and satellite clock offsets, respectively; $b^{s,i}, b_{r,i}$ ($i = 1,2$) are the instrument delays in units of ns from GNSS satellite *s* and onboard receiver *r* at two frequencies, respectively; *c* is the light speed in vacuum; $P_{r,GF}^s$ is the geometry-free combination of pseudorange observations in meters; STEC is the slant total electron content of the topside ionosphere or plasmasphere in units of TECU; $\alpha_1, \alpha_2, \alpha$ are the coefficients of the STEC in units of m/TECU that relates to GPS L1 and L2 frequencies; $\text{DCB}^s, \text{DCB}_r$ denote the GNSS satellite *s* and receiver *r* DCB values in units of meter, respectively; $\varepsilon_{r,i}^s, \varepsilon_{r,GF}^s$ are the noise from pseudorange observations and their GF combination observations.

The slant total electron content (STEC) is defined as the product of VTEC and a mapping function *mf*. For mapping functions, GNSS-derived ionosphere models are usually based on the so-called single-layer model (SLM) as outlined. This model assumes that all free electrons are concentrated in a shell of infinitesimal thickness and are described by a function of geomagnetic latitude and sun-fixed longitude (Schaer 1999; Yuan 2002; Yuan et al. 2017). The height of the idealized layer is usually set to the expected height of the maximum electron density, which is called the ionospheric effective height (IEH) (Zhong et al. 2015a). Wautelet et al. (2017) compared the geometric mapping function of Xu (2003) with the SLM mapping function for LEO-based DCB estimation, and he pointed out that both solutions were equivalent in terms of error bars. A function called the F&K mapping function (Foelsche and Kirchengast 2002) originally developed for converting slant-path atmospheric water vapor to the vertical retrieved was applied to LEO-based TEC conversion (Yue et al. 2011). The F&K mapping function is

a thick layer model with the layer thickness of IEH above the receiver. Zhong et al. (2016) illustrated that the F&K mapping function together with the IEH was more suitable for LEO-based TEC conversion under certain conditions, though the SLM was more appropriate for the ground-based vertical TEC retrieval. Yue et al. (2011), Lin et al. (2014), Li et al. (2017a) and Li et al. (2019) applied the F&K geometric mapping function to complete the conversion from slant to vertical plasmasphere delay. In this study, we employed the F&K mapping function to convert the plasmasphere TEC, and the LEO-based VTEC has been modeled and expressed in the form of a spherical harmonic function to improve its temporal and spatial resolution. Here, we described the ionospheric pierce point (IPP) as the intersection of IEH and the slant signal ray path. Using the LEO-based VTEC models, the onboard data from different orbit heights could be applied to solve satellite DCBs, and the global plasmasphere VTEC was modeled in a solar-geomagnetic reference frame using a spherical harmonic expansion up to degree and order of 12 in our study. The temporal modeling mode was set to dynamic status, with the time spacing set to 12 h for LEO onboard observations. The relationship between STEC and VTEC can be expressed as shown in (3):

$$\begin{cases} \text{STEC} = mf_{F\&K} \cdot \text{VTEC} \\ mf_{F\&K} = \frac{1 + (R_E + h_{IEH})/R_{LEO}}{\cos z + \sqrt{(R_E + h_{IEH})^2/R_{LEO}^2 - (\sin z)^2}} \\ h_{IEH} = (0.0027F_{107} + 1.79)h_{LEO} - 5.52F_{107} + 1350 \\ \text{VTEC} = \sum_{n=0}^{n_{\max}} \sum_{m=0}^n \tilde{P}_{nm}(\sin \varphi) \cdot (\tilde{A}_{nm} \cos(m\lambda) + \tilde{B}_{nm} \sin(m\lambda)) \end{cases} \quad (3)$$

where STEC and VTEC represent the slant and vertical total electron content of the topside ionosphere or plasmasphere in units of TECU; $mf_{F\&K}$ refers to the F&K mapping function, R_E is the earth radius in kilometers; h_{IEH} represents the IEH in kilometers; here, $R_{LEO} = R_E + h_{LEO}, h_{LEO}$ denotes the orbit height of LEO satellite above the earth's surface in units of kilometer, F_{107} is the solar radio flux at 10.7 cm, and z is the zenith angle of the slant ray path. In the expression of VTEC, φ and λ are, respectively, the geographic latitude and the sun-fixed longitude, n_{\max} is the maximum degree of the spherical harmonic expansion; \tilde{P}_{nm} is the normalized associated Legendre functions of degree *n* and order *m*; $\tilde{A}_{nm}, \tilde{B}_{nm}$ are the estimated TEC coefficients of the spherical harmonic function.

As satellite and receiver DCBs are closely correlated, resulting in normal matrix rank deficiency, the DCB datum is defined by a zero-mean condition that is imposed on the

satellite bias estimation for decorrelation. The zero-mean condition can be written as shown in (4):

$$\sum_{s=1}^{S_{\max}} \text{DCB}^s = 0 \quad (4)$$

where S_{\max} refers to the total number of observed navigation satellites.

The larger the elevation cutoff angle, the greater the correlation between the VTEC and receiver DCBs, so the ideal elevation angle is low enough to allow VTEC and receiver DCB estimation decorrelation. In order to make use of onboard observations, a sample interval of 10 s and cutoff elevation of 15° were adopted for onboard data. The cutoff elevation angle of 15° is applied based on the fact that the GPS antenna is tilted by 15° with respect to the JASON satellite X/Z plane (Cerri et al. 2010; Wautelet et al. 2017). In this case, the minimum 0° can reduce multipath error and measurement noise to some extent. The daily DCB values should be realigned by applying a shift from non-all satellite DCB, which can be computed using a common set of satellites over the period of interest.

After applying the alignment procedures, we compared and evaluated results from the different DCB schemes, taking comparison with their respective stability (Zhong et al. 2015b; Sanz et al. 2017) as internal evaluation and comparisons with the external reference products as external evaluation. GPS satellite DCBs were evaluated using internal and external evaluation. Internal evaluation refers to estimated DCBs monthly stability analysis, provided in the form of standard deviation (STD), while external evaluation contains the difference mean and standard deviations and difference root mean square (RMS) for estimated DCB values with respect to CODE daily products (Schaer 1999), given in the form of different GPS satellite.

The monthly stability of satellite DCBs, provided in the form of STD, can reflect the stability and reliability of DCB estimation to some extent, and it is expressed as follows:

$$\text{STD}^s = \sqrt{\frac{\sum_{d=1}^{dd} (b_d^s - \bar{b}^s)^2}{dd - 1}} \quad (5)$$

where the superscript s and d represent the navigation satellite and day of a month, respectively, STD^s denotes the monthly stability of the navigation satellite s DCB values, b_d^s is the estimated DCB values of satellite s on day d in a month, \bar{b}^s refers to the monthly mean of the satellite s DCB values estimated, and dd represent the total days of the month.

After applying the alignment procedures, the differences RMS values for estimated GPS satellite DCBs relative to

external reference products, given in the form of different GPS satellites, are calculated according to the following:

$$\text{RMS}^s = \sqrt{\frac{\sum_{d=1}^{dd} (b_d^s - \tilde{b}_d^s)^2}{dd}} \quad (6)$$

where the superscript dd represents the total days of the month; RMS^s denotes the difference RMS of the GNSS satellite s DCB values with respect to the reference products; b_d^s is the estimated DCB values of satellite s on day d in a month; \tilde{b}_d^s refers to the satellite s DCB values of the external reference products on day d .

2.2 The innovations in DCB processing strategies

There are two important differences in estimation strategies. The first lies in terms of the data preprocessing method. In most studies, DCB estimation based on onboard and ground data uses the carrier-to-code leveling process. Due to more cycle slips in the onboard phase observations compared to ground data, larger error is easily introduced by carrier-to-code leveling. We made DCB estimation procedures using clean onboard code observations, which are screened by LEO satellite precise orbits calculated from phase observations. Before carrying out the LEO-based DCB estimation, we conducted some data preprocessing procedures for the space-borne observation to obtain clean code observation. In a first step, code observations were screened iteratively by single point positioning (SPP) epoch solution in the form of ionosphere-free combination observations, and outlier observations detected with RMS of kinematic solution. After that, the high-accuracy LEO orbits as known prior orbit information derived from the phase observations were introduced into SPP epoch estimation equations. A second screening for code observations was conducted iteratively using the estimation residuals of 10 m and confidence interval of 5 sigma. Finally, the cleaner code data were used to calculate DCB values. This preprocessing for pseudorange draws on the data preprocessing method of LEO precise orbit determination (Kang et al. 2006; Liu et al. 2019). In this way, the pseudorange obtained by this method is relatively clean. In addition, it should be noted that DCB estimation applied LEO orbits as prior orbits, calculated by reduced-dynamic precision orbit determination (Kang et al. 2006; Liu et al. 2019).

The second difference was that we proposed an ionosphere processing method for LEO-based DCB estimation using onboard data from different orbit heights. First, the plasmasphere of the slant ray path was modeled based on F&K mapping function and spherical harmonic function, to obtain the LEO-based VTEC model. It contribute to improve VTEC temporal and spatial resolution. Then, we jointly estimated the available LEO data from different orbit heights,

by introducing two LEO-based VTEC models to remove its effects—it having been derived from the modeling results of paired LEO data at the same orbital height, respectively. The DCB estimation models based on onboard data of n LEO satellites at the same [Eq. (7)] and different orbit heights [Eq. (8)] can be written as:

$$\begin{cases} P_1 = \alpha \cdot m_{f_1} \cdot VTEC_i + DCB^G + DCB_{r1} \\ P_2 = \alpha \cdot m_{f_2} \cdot VTEC_i + DCB^G + DCB_{r2} \\ \dots \\ P_n = \alpha \cdot m_{f_n} \cdot VTEC_i + DCB^G + DCB_{rn} \end{cases} \quad (7)$$

$$\begin{cases} P_1 = \alpha \cdot m_{f_1} \cdot VTEC_1 + DCB^G + DCB_{r1} \\ P_2 = \alpha \cdot m_{f_2} \cdot VTEC_2 + DCB^G + DCB_{r2} \\ \dots \\ P_n = \alpha \cdot m_{f_n} \cdot VTEC_n + DCB^G + DCB_{rn} \end{cases} \Rightarrow \begin{pmatrix} P_1 - \alpha \cdot m_{f_1} \cdot VTEC_1 \\ P_2 - \alpha \cdot m_{f_2} \cdot VTEC_2 \\ \vdots \\ P_n - \alpha \cdot m_{f_n} \cdot VTEC_n \end{pmatrix} = \begin{pmatrix} 1 & 10 & \dots & 0 \\ 101 & \dots & 0 \\ \vdots & \ddots & \\ 100 & \dots & 1 \end{pmatrix} \cdot \begin{pmatrix} DCB^G \\ DCB_{r1} \\ DCB_{r2} \\ \vdots \\ DCB_{rn} \end{pmatrix} \quad (8)$$

where the subscripts of $G, 1, 2, \dots, n$, respectively, represent GPS satellites and $1, 2, \dots, n$ LEO satellite receivers; the subscript of i denotes a certain VTEC value; other symbols are the same as the above section. The $VTEC_i$ in the Eq. (8) can be derived from the Eq. (7).

3 Experiments and results

We applied onboard observations from four LEOs at two different orbit heights to estimate DCB products; among the satellites, GRACE-A and -B have orbit altitudes of 400 km, and the orbits of the JASON-2 and -3 above the ionosphere are at the altitude of 1350 km; so clearly, their parameter settings for LEO-based VTEC modeling were different from each other. The prior IEH heights for GRACE-A/B and JASON-2/3 satellites were set at 1500 km and 3500 km, respectively, according to Eq. (3). In this section, we present the research results related to one month of onboard data: from day-of-year (DOY) 183 to 213 in 2016.

In the first step, DCBs values and plasmasphere parameters were simultaneously calculated using just a single LEO satellite to test the reliability of estimation method. We then employed paired LEO satellites data from the same orbit heights to estimate satellite and receiver DCBs, together with modeling the LEO-based VTEC. After that, estimation schemes of 2–4 LEO satellites at two different orbital planes have been built by introducing two LEO-based VTEC models of the above step, and their stability and accuracy were also analyzed. Below, the estimation results have been shown, and the LEO-based plasmasphere VTEC models have also been simply evaluated. Based on the these experiment results, we

have presented some conclusions in relation to GPS satellite DCB estimation based on LEO onboard data.

3.1 DCB estimation using a single LEO satellite data

In this section, onboard GNSS observations from four LEO satellites (GRACE-A and -B and JASON-2 and -3) were used to estimate DCB values one-by-one, respectively. The GPS satellite DCBs, onboard receiver DCBs and LEO-based VTEC parameters were simultaneously estimated based on single LEO onboard data. After aligning the estimated results, GPS satellite DCBs were evaluated from internal

(monthly stability) and external (difference mean, standard deviations and RMS) aspects evaluation. Receiver DCBs were evaluated only using internal stability due to lack of reference products. DCB values for G04 were not estimated due to a lack of observations.

3.1.1 Satellite DCB estimation and accuracy analysis

Figure 1 displays the monthly stability of GPS satellites DCBs based on data from single LEO satellite; the satellite DCB monthly STD mean is listed in Table 1, including the results of CODE products (Schaer 1999) and DLR products (Montenbruck et al. 2014) using the different estimation methods. The monthly STD in Table 1 means monthly stability. We can also see that most GPS satellite DCBs are within 0.15 ns based on individual LEO satellite in Fig. 1. The similarity in GPS satellite DCB monthly STD mean is also evident in the values listed in Table 1, where it can be seen that the monthly STD mean values for GRACE-A and -B, and JASON-2 and -3 are 0.097, 0.099, 0.092, and 0.094 ns, respectively. The monthly STDs mean values for CODE and DLR are 0.023 and 0.065 ns, showing that the DCB stability for single LEO satellite solutions is worse than that of CODE and DLR products.

We take CODE DCB daily products as a reference of external evaluation (Schaer 1999). Mean difference and STD for GPS DCBs relative to CODE products using single LEO data are shown in Fig. 2. Figure 3 depicts the differences RMS in GPS satellites DCBs between single LEO schemes and CODE products, provided in the form of different GPS satellites. Compared with CODE products, the differences mean

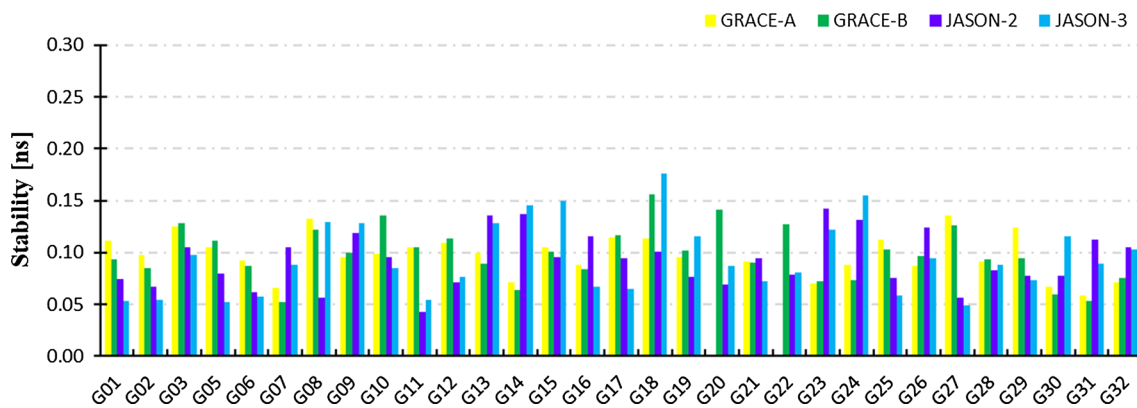


Fig. 1 GPS satellites DCBs monthly stability based on single LEO satellite data. The yellow column, green column, dark blue column, and lake blue column represent monthly stability obtained from GRACE-A, -B, JASON-2, -3 satellites, respectively

Table 1 Statistics for monthly STD mean for GPS satellite DCBs

With	STD mean (ns)	With	STD mean (ns)
GRACE-A	0.097	JASON-2	0.092
GRACE-B	0.099	JASON-3	0.094
CODE	0.023	DLR	0.065

for GPS DCBs based on GRACE-A and -B, and JASON-2 satellite data vary between -0.4 and 0.4 ns, while the difference of JASON-3 data is larger than others, approximately within 0.6 ns. According to statistics, the standard deviations of difference for GPS DCBs are within 0.18 ns based on single LEO satellite data. In Fig. 3, RMS time series for different GPS satellite DCB differences between the estimated DCBs and CODE products are within 0.6 ns, and the corresponding difference RMS for JASON-3 is slightly worse than that of the others. According to the statistics, the difference RMS mean values for GPS DCBs using single LEO solutions (GRACE-A, -B, JASON-2, -3 satellites) are 0.192 , 0.204 , 0.200 , 0.225 ns, respectively. We can see that the mean difference and its RMS mean for JASON-3 are slightly worse than the others, and it may be related to data quality. In addition, the JASON-3 satellite was launched in January 2016, and the data selected in the study were July 2016. We have compared the positioning accuracy using pseudorange observations of JASON-3 and other satellites. As shown in Fig. 4, it was found that the RMS of unit weight of SPP estimation using pseudorange data of LEO satellites is also worse than that of others using the same estimation method, and mean values for RMS of unit weight using GRACE-A, -B, and JASON-2, -3 satellites are 0.58 , 0.64 , 1.12 , and 2.02 m, respectively. It shows that the data quality of JASON-3 satellite may be not as good as that of other satellites in the same period, resulting in the relatively poor results for the JASON-3 satellite.

3.1.2 Receiver DCB estimation

Mean and STD for onboard receiver DCBs using single LEO satellite schemes are listed in Table 2, where it can be seen that onboard receiver DCBs for the GRACE-A and -B and JASON-2 and -3 satellites are -19.224 ± 0.144 , -14.653 ± 0.132 , -2.584 ± 0.165 , and -8.794 ± 0.264 ns, respectively. The STD for GRACE-A and -B and JASON-2 receiver DCBs are better than that results calculated for JASON-3, similar results obtained for the GPS satellite DCB daily difference RMS. The reasons may also be related to data quality of JASON-3 observations described in Sect. 3.1.1. In addition, it has already been suggested that space-based receiver DCBs may depend on the receiver temperature (Yue et al. 2011), but now we cannot obtain the temperature data of onboard receivers, and their relationship need to be further investigated.

3.2 DCB estimation using two LEO satellites data from the same orbit altitude

In order to improve estimation accuracy and to model the topside ionosphere or plasmasphere delay better, we take LEO satellites into the GRACE-A and -B, and JASON-2 and -3 two schemes, with the each set of two LEO satellites (paired satellites) at the same orbital altitude. In the two schemes, the obtained LEO-based VTEC values differ from each other due to their different altitudes. The obtained estimation results for the GPS satellite and receiver DCBs using two paired LEO satellite data are analyzed; the LEO-based

Fig. 2 Mean difference and standard deviations for GPS DCBs with respect to CODE products using single LEO data. Dots denote the GPS DCB difference mean, and the length of the vertical lines denotes the respective standard deviations

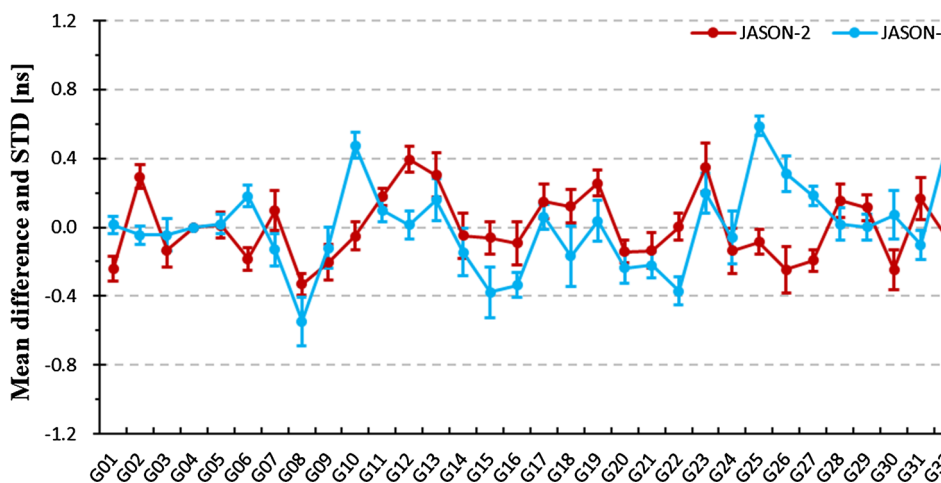
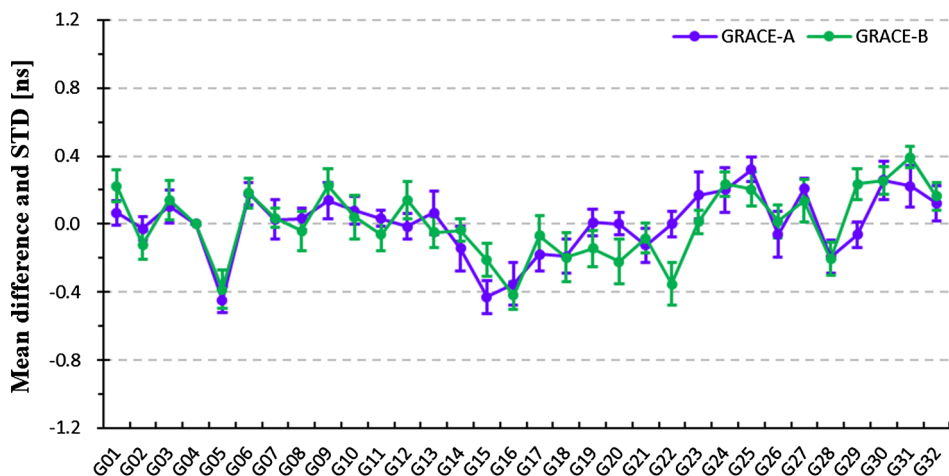
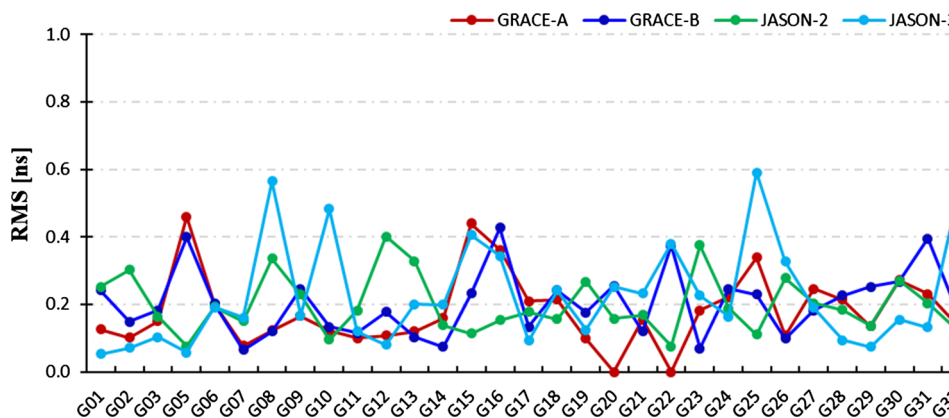


Fig. 3 RMS for GPS satellite DCB differences between single LEO solutions and CODE products, given in the form of different GPS satellites. The red line, dark blue line, green line, and lake blue line represent RMS time series obtained from GRACE-A, -B, JASON-2, -3 satellites data, respectively



plasmasphere VTECs are modeled using onboard data from the same orbit height.

3.2.1 Satellite DCB estimation and accuracy analysis

The GPS satellites DCB monthly stabilities using two sets of paired LEOs at their respective heights, including the

GRACE-A and -B, and JASON-2 and -3 schemes, are illustrated in Fig. 5. As can be seen in Fig. 5, GPS satellites DCB monthly stabilities range between 0.05 and 0.15 ns, and estimated DCB values based on JASON-2 and -3 are more stable than those for GRACE-A and -B. According to statistics, the monthly STD mean values for two schemes involving GRACE and JASON satellites are 0.095 and 0.079 ns, and

Fig. 4 RMS of unit weight based on SPP estimation using pseudorange data of LEO satellites. The blue dots, red dots, green dots, and lake blue dots represent RMS values of unit weight using GRACE-A, -B, and JASON-2, -3 satellites data, respectively

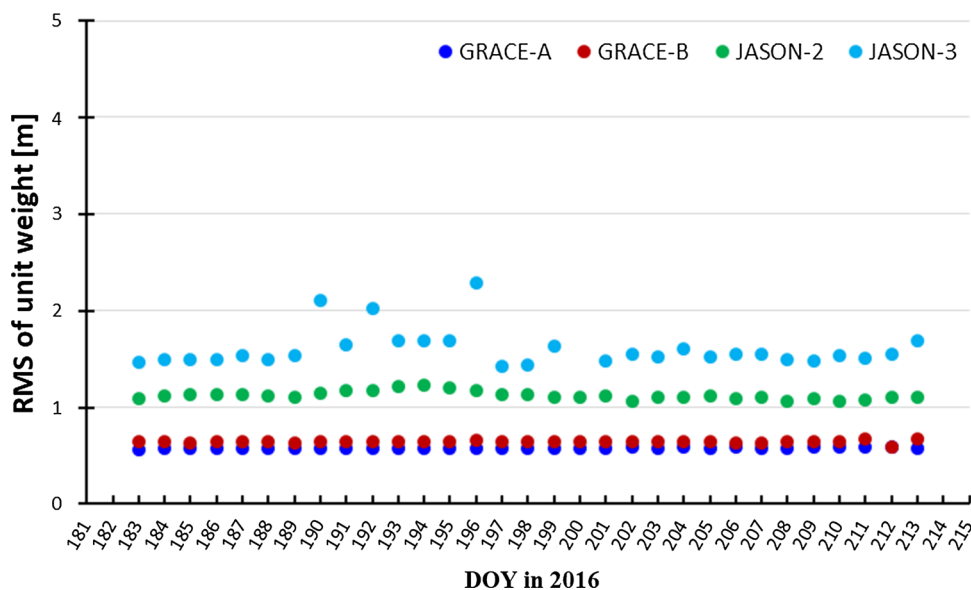
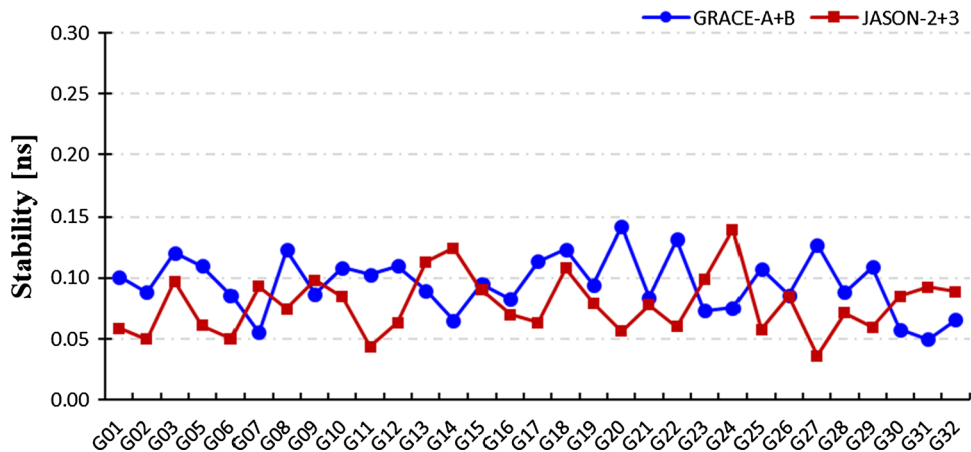


Table 2 Mean and STD statistics for onboard receiver DCBs from single LEO data solutions

Receiver	Mean (ns)	STD (ns)
GRACE-A	- 19.224	0.144
GRACE-B	- 14.653	0.132
JASON-2	- 2.584	0.165
JASON-3	- 8.794	0.264

Fig. 5 GPS satellites DCB monthly stabilities derived from two paired LEO data from the same altitude. The blue line and red line represent the time series for monthly stabilities obtained from GRACE-A and -B paired satellites solution and JASON-2 and -3 paired satellites solution, respectively



that these results are slightly superior to the results obtained using single LEO satellite solutions from Table 1.

Figure 6 depicts the mean difference and standard deviations for GPS DCBs relative to CODE products using paired LEOs data, and Fig. 7 shows the corresponding DCB differences RMS with respect to CODE products.

The mean differences of GPS satellite DCBs using paired LEOs data relative to CODE products all vary between - 0.4 and 0.4 ns, and the corresponding standard deviations of differences are within 0.14 ns. The DCBs differences RMS for different GPS satellites, based on paired LEOs are in the range of 0–0.4 ns. Statistically, RMS mean from Fig. 7 using

GRACE-A plus -B paired satellites and JASON-2 plus -3 paired data are 0.196 and 0.168 ns, respectively. Compared with single LEO solutions, it can be found that the RMS for the JASON-2 plus -3 scheme is superior to that established for the single LEO satellite solutions, and that the difference RMS mean based on GRACE-A plus -B scheme is superior to that for the GRACE-B solution and similar to the accuracy of GRACE-A solution.

Fig. 6 Mean difference and standard deviations for GPS DCBs relative to CODE products using paired LEOs data. Dots denote the GPS DCB difference mean, and the length of the vertical lines denotes the respective standard deviations

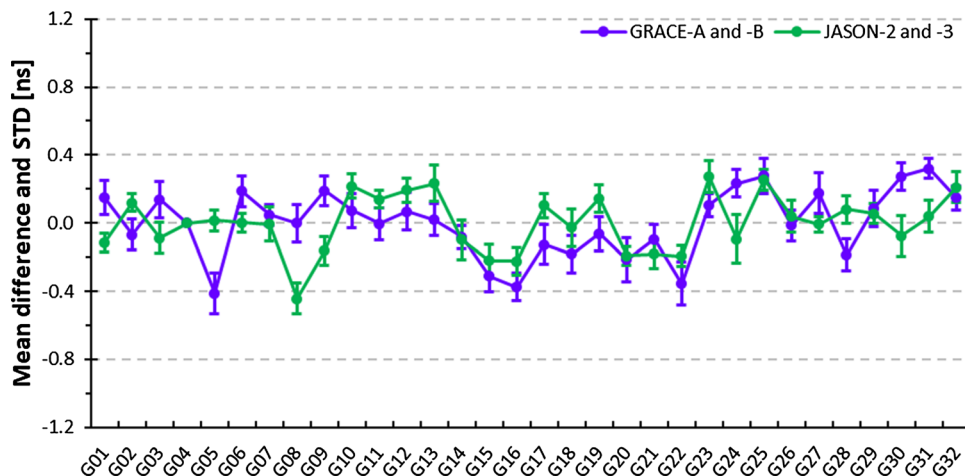
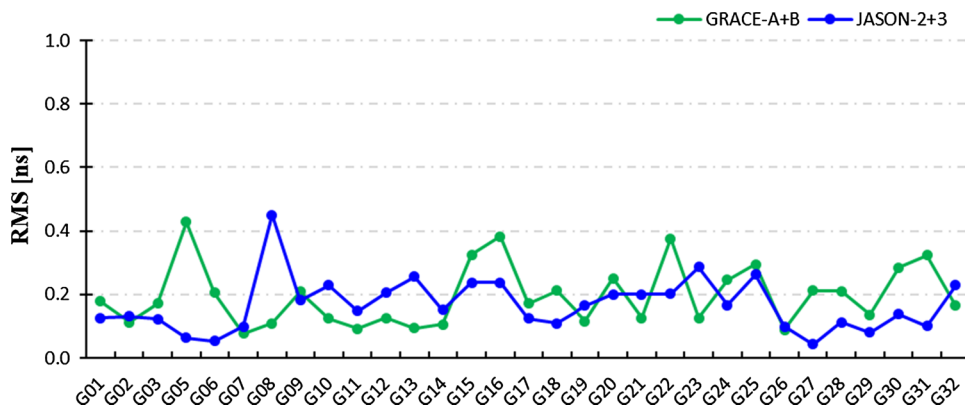


Fig. 7 GPS satellite DCB differences RMS based on paired LEOs solutions with respect to CODE products, given in the form of GPS satellites. The green line and blue line represent RMS time series obtained from schemes GRACE-A and -B paired satellites, JASON-2 and -3 paired satellites, respectively



3.2.2 Receiver DCB estimation

Means and STD for onboard receiver DCBs are displayed in Table 3. We can see that the receiver DCBs stabilities for GRACE-A and -B paired scheme are both 0.128 ns, showing some improvement compared with the single LEO satellite schemes. It can be seen that stabilities for the JASON-2 and -3 scheme are 0.198 and 0.199 ns, superior to that of single JASON-3 solution. In Table 3, STDs for paired LEO satellites are almost identical in each set solution. The reasons may be that the paired LEO satellites, such as GRACE-A and -B or JASON-2 and -3, have the same high-accuracy receivers and similar ionosphere activity characteristics due to similar satellite tracks that the paired receivers experienced.

3.3 DCB estimation using more than two LEO satellites data from different orbit heights

In order to make full use of available LEO onboard data from different orbital altitudes, we designed three schemes for GPS satellite DCB estimation—GRACE-A and JASON-2 (two satellites), GRACE-A and -B and JASON-2 (three satellites), and GRACE-A and -B plus JASON-2 and -3 (four satellites); these three schemes capture different topside iono-

Table 3 Mean and STD statistics for receiver DCBs

Receiver	Mean (ns)	STD (ns)
(a)		
GRACE-A	- 19.330	0.128
GRACE-B	- 14.968	0.128
(b)		
JASON-2	- 2.562	0.198
JASON-3	- 9.003	0.199

(a) The mean and STD for receiver DCBs obtained from paired GRACE satellites solution, and (b) the mean and STD using paired JASON satellites data

sphere or plasmasphere VTECs from GPS satellites to LEOs at different orbit heights. In this case, we propose and apply the two LEO-based VTEC models estimated in Sect. 3.2 to deduct the plasmasphere VTEC delay. We evaluate the stability and accuracy of DCB estimation based on onboard data of three schemes from different orbit heights.

3.3.1 Satellite DCB estimation and accuracy analysis

During both the two schemes for GRACE-A plus JASON-2, and GRACE-A and -B plus JASON-2, we select the JASON-

Fig. 8 Time series of daily GPS satellite DCBs using four LEO satellites solution

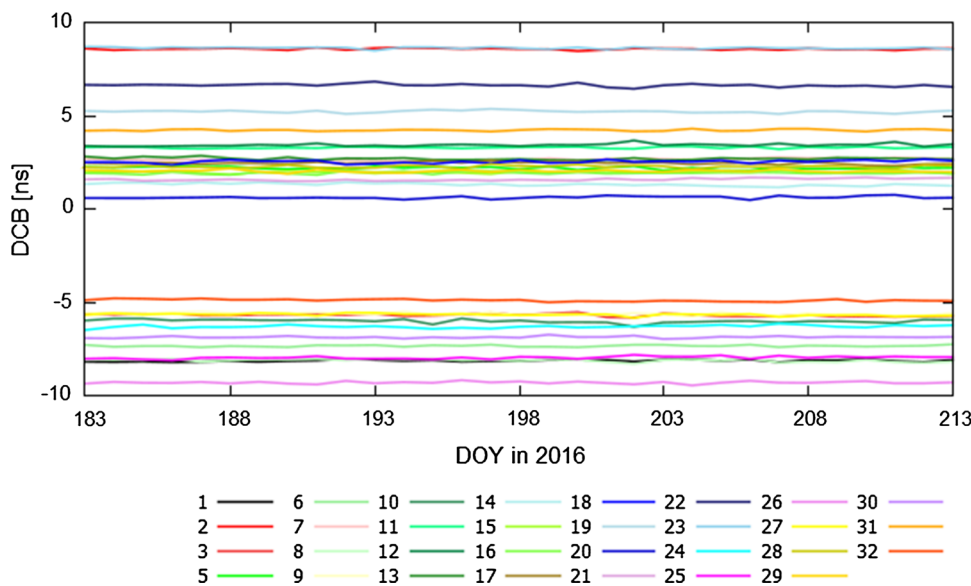
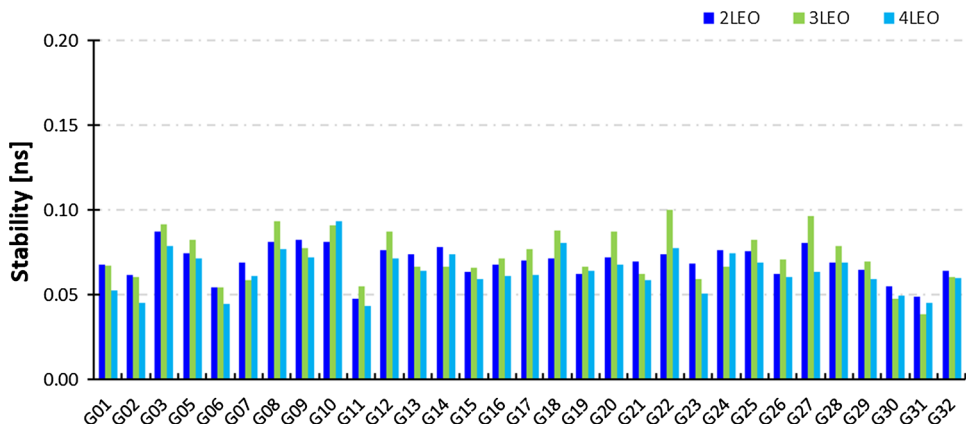


Fig. 9 Monthly stability for GPS satellite DCBs using more than two LEO satellites at different orbit heights. The dark blue column, green column, and lake blue column represent the monthly stabilities obtained from GRACE-A and JASON-2 satellites solution, GRACE-A and -B and JASON-2 satellites solution, and GRACE-A and -B, JASON-2 and -3 satellites solution, respectively



2 onboard data to test due to its higher accuracy compared with JASON-3 data. The time series for daily GPS satellite DCBs using four LEO data from different orbit heights are shown in Fig. 8, where it can be seen that GPS satellite DCB values range between -10 and 10 ns and are relatively stable. The monthly stability for GPS satellites DCBs using more than two LEO satellites data from different orbit heights is presented in Fig. 9. Table 4 lists the STD mean for corresponding GPS satellite DCBs, for the sake of convenient comparison, also showing the results of LEO estimation schemes in Sects. 3.1 and 3.2. As shown in Fig. 9, the GPS DCBs stability using four LEO satellites data is mainly $0.04\text{--}0.10$ ns. The GPS satellite DCBs stability using four LEOs solution is similar to that of the DLR products (0.065 ns), and the CODE products have highest monthly stability (0.023 ns). The monthly stability achieved using multi-LEOs data is better than that of single LEO schemes. The stability of 0.064 ns based on four LEO satellites data is optimal in the all tested LEO solutions, manifesting that the more the number of LEO satellites involved, the higher

the monthly stability achieved. Compared with single LEO satellite solutions, the GPS DCB monthly stability using two LEOs (GRACE-A and JASON-2), three LEOs (GRACE-A and JASON-2 and -3), and four LEOs data are approximately improved by $25\text{--}35\%$. The estimated DCB results based on GRACE-A and JASON-2 satellites data from different orbit heights are more stable than those achieved by the GRACE-A and -B or JASON-2 and -3 schemes from the same height, due to removing the LEO-based plasmasphere VTEC effects.

Figure 10 shows the mean difference and standard deviations for GPS DCBs compared with CODE products, using multi-LEOs data from different orbit heights. Meanwhile, the monthly DCB differences RMS for different GPS satellites with respect to CODE products, using multi-LEOs data from different orbit heights, are displayed in Fig. 11. The DCB differences RMS mean statistics from Fig. 11 are shown in Table 5, involving RMS results of all tested LEO satellite solutions for convenient comparison. It can be found that the time series for the mean difference of GPS DCB using

Fig. 10 Mean difference and standard deviations for GPS DCBs relative to CODE products using multi-LEOs data from different orbit heights. The green dots, blue dots, and red dots represent results obtained from GRACE-A plus -B satellites data, GRACE-A plus -B plus JASON-2 satellites data, GRACE-A plus -B plus JASON-2 plus JASON-3 satellites data, respectively

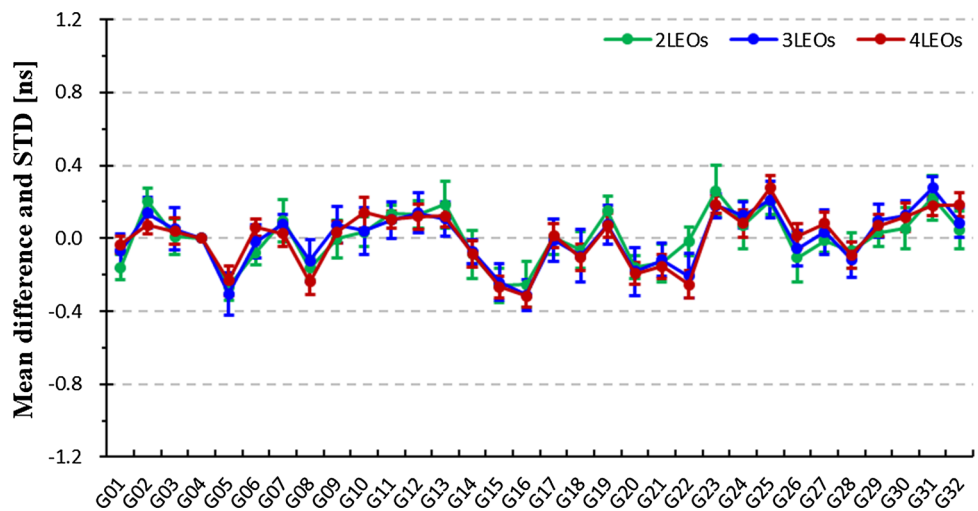


Fig. 11 GPS satellite DCB differences RMS using multi-LEO satellites data from different orbit heights with respect to CODE products. The red line, green line, and blue line represent RMS time series obtained from schemes GRACE-A and JASON-2 satellites, GRACE-A and -B and JASON-2 satellites, GRACE-A and -B and JASON-2 and JASON-3 satellites, respectively

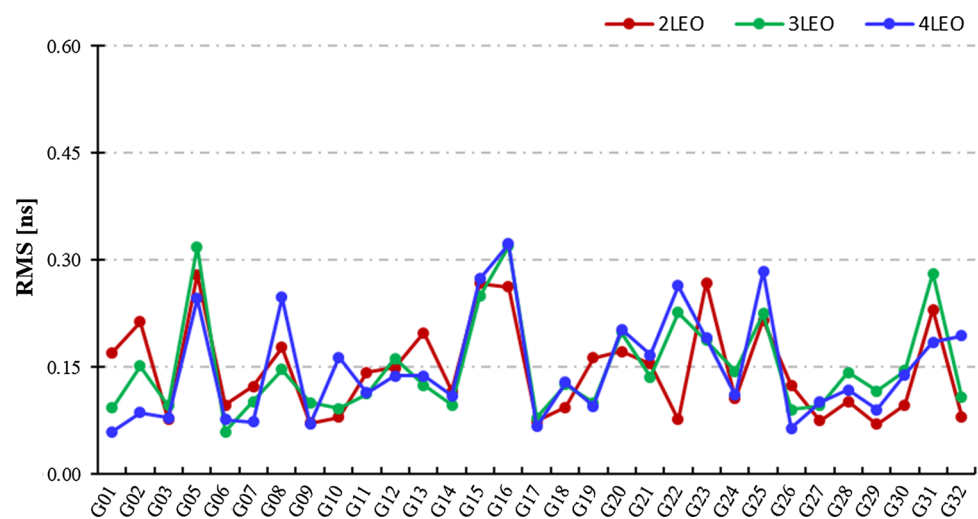


Table 4 Monthly STD mean for GPS satellite DCBs

With	STD mean (ns)
GRACE-A	0.097
GRACE-B	0.099
JASON-2	0.092
JASON-3	0.094
GRACE-A and -B	0.095
JASON-2 and -3	0.079
GRACE-A and JASON-2	0.070
GRACE-A and -B and JASON-2	0.072
4LEOs	0.064

multi-LEOs data from different orbit heights are smoother than other single LEO schemes or paired LEOs solutions, and related standard deviations are within 0.10 ns, which are superior to that of single LEO solutions within 0.18 ns, and of paired LEOs solutions within 0.14 ns. According to statistics, mean values of difference standard deviations are

improved by more than 30% compared with single LEO solutions. We can see that the DCB differences RMS compared with CODE products are within 0.3 ns, approximately, which are superior to that of single LEO solutions within 0.6 ns and of paired LEOs solutions within 0.4 ns. It is obvious that the schemes GRACE-A and JASON-2 (two LEOs) of 0.146 ns, the GRACE-A and -B and JASON-2 (three LEOs) of 0.149 ns, and four LEOs of 0.148 ns exhibit better accuracies than the other solutions. It also indicates that the accuracy of GPS satellite DCBs using multi-LEOs data from different orbit heights is superior to that from either the same orbital height or single LEO satellite solutions. Compared with the difference RMS of single LEO solutions, the RMS accuracies for schemes GRACE-A and JASON-2 (two LEOs), the GRACE-A and -B and JASON-2 (three LEOs), and four LEOs are improved by 25–35% approximately. Among all the schemes, the best stability is obtained using four LEO satellites data from different orbit heights, with GPS satellite DCB stability of 0.064 ns; the optimal accuracies of

Table 5 RMS mean statistics for GPS satellite DCB differences based on multi-LEO schemes relative to CODE products

Satellite	RMS mean (ns)
GRACE-A	0.192
GRACE-B	0.204
JASON-2	0.200
JASON-3	0.221
GRACE-A and -B	0.196
JASON-2 and -3	0.168
GRACE-A and JASON-2	0.146
GRACE-A and -B and JASON-2	0.149
4LEOs	0.148

DCB estimation are approximately the scheme GRACE-A and JASON-2 (two LEOs) of 0.146 ns.

In general, the number of satellites and the plasmasphere VTEC affected GPS satellite DCB accuracy. For LEO satellites at the same orbit heights, when LEO satellite orbits are low at the height of high electron density—such as GRACE-A and -B satellite—the two LEO satellites play a little role for accuracy improvement. When LEO orbits are above the high electron density area, such as JASON-2 and -3 satellite, the number of LEO satellites involved has an impact on the accuracy of DCB estimation. It is clear that the more onboard data involved, the more stable the estimation results. After removing the plasmasphere delay for LEO satellites at different heights, it seems that the number of LEO satellites has little effect on GPS DCB estimation accuracy, although we can still see that more available LEO onboard data provide more stable estimation results.

3.3.2 Receiver DCB estimation

Figure 12 shows the time series of onboard receiver DCBs achieved using four LEO data in July 2016. Table 6 lists the mean and STD statistics for receiver DCBs from the results plotted in Fig. 12. The receiver DCBs are mainly in the range of -20 to 0 ns, and it can be seen that the JASON-3 receiver DCBs fluctuations are slightly larger than those for the others. Comparing Table 6(b)–(d), it can be seen that the receiver DCB STD for the same type of LEO satellites at the same orbit heights is almost identical, using the different LEO satellites data from different orbit heights, which the receiver DCB STD based on GRACE series satellites, and JASON series satellites are 0.135 and 0.197 ns, respectively. The multi-LEO satellites solution used more observation data and more stable topside ionosphere models, which is more stable and accurate than that based on single LEO satellite data. The STD value of JASON-3 receiver DCB is larger than others, while the single LEO satellite solution is easily affected by many factors, such as data quality or receiver tem-

Table 6 Mean and STD statistics for onboard receiver DCBs

Receiver	Mean (ns)	STD (ns)
(a)		
GRACE-A	-19.224	0.144
GRACE-B	-14.653	0.132
JASON-2	-2.584	0.165
JASON-3	-8.794	0.264
(b)		
GRACE-A	-19.039	0.133
JASON-2	-2.566	0.196
(c)		
GRACE-A	-19.047	0.133
GRACE-B	-14.693	0.134
JASON-2	-2.572	0.196
(d)		
GRACE-A	-19.056	0.133
GRACE-B	-14.698	0.135
JASON-2	-2.573	0.197
JASON-3	-9.013	0.197

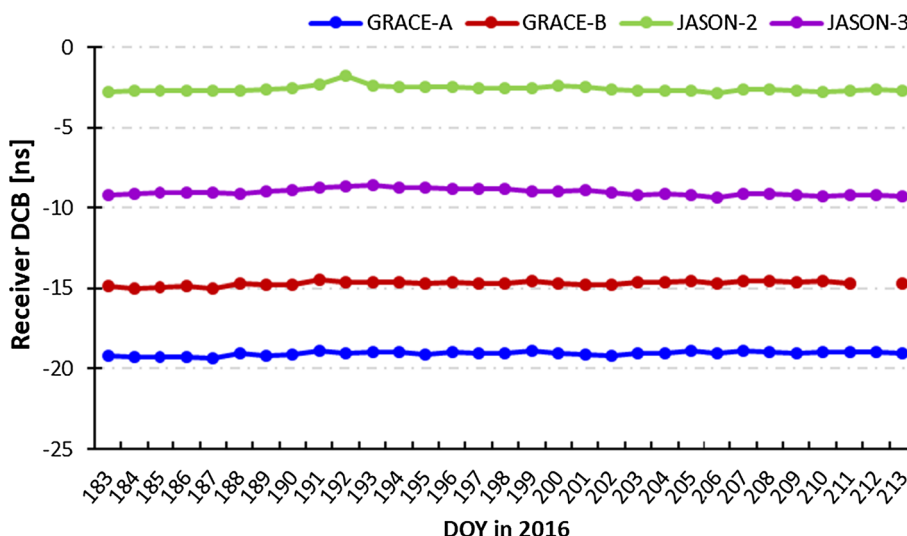
(a) The mean and STD for receiver DCBs using single LEO satellite schemes, (b) the mean and STD obtained from GRACE-A and JASON-2 satellites scheme, (c) the mean and STD obtained from GRACE-A and -B and JASON-2 satellites scheme, and (d) the mean and STD using four LEO satellites scheme

perature, and JASON-3 receiver DCB is also easily affected.

3.4 LEO-based plasmasphere VTEC analysis

During DCB estimation using two paired LEO data from the two different orbit height planes, the LEO-based plasmasphere VTEC was also obtained and refined. In Sect. 3.3, we worked DCB estimation by introducing two LEO-based TEC models derived from two paired satellites data (from Sect. 3.2), to remove the upper ionosphere effects. Different for the specific assessments methods of ground-based ionosphere VTEC (Hernández-Pajares et al. 2017; Li et al. 2017b), we only performed a simple evaluation for the accuracy and stability of the obtained plasmasphere VTEC due to the length of the paper. To verify the reliability of plasmasphere VTEC, we firstly, added the estimated LEO-based VTEC and International Reference Ionosphere (IRI) 2016 model, which the IRI model had been derived from a large amount of ionosphere detection data (Bilitza 2009; Bilitza et al. 2017). The IRI 2016 model adds Shubin model option for ionosphere F2 peak height calculation. IRI_Shubin model was built using the observation data from three occultation missions (CHAMP/GRACE/COSMIC) and global observation from 62 ionosondes from 1987 to 2012 (Bilitza et al. 2017). To obtain better performance of IRI 2016 outputs, we

Fig. 12 Onboard receiver DCB time series from the four LEOs solution



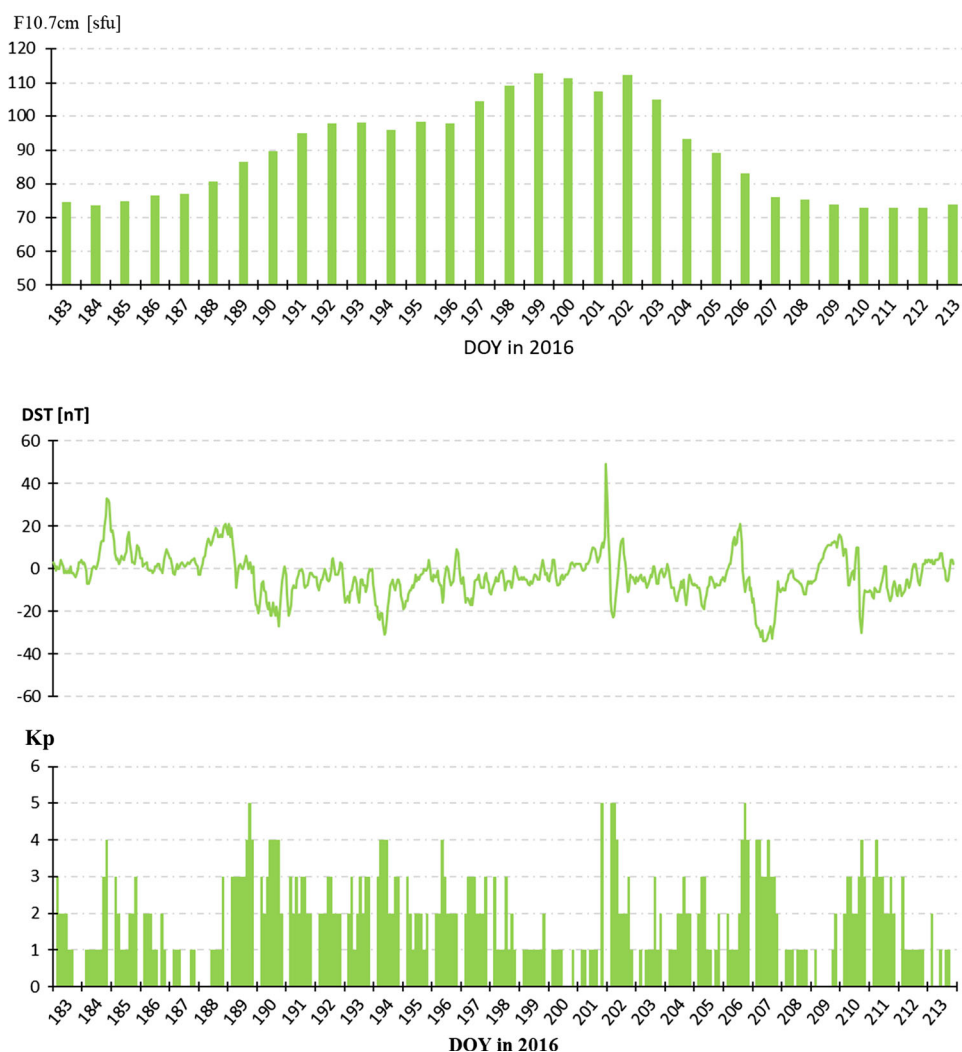
selected the IRI_Shubin option in the manuscript. Then, we compared the above summed VTEC with the CODE Global Ionosphere Map (GIM) (Schaer 1997, 1999) and analyzed the reliability of the estimated LEO-based VTEC models. Before this work, we analyzed the corresponding geomagnetic and solar conditions.

The time series for solar and geomagnetic indices on July 2016 are shown in Fig. 13. The solar activity index on DOY 183 is 74.5 sfu, which indicated that there is not an active solar activity level on this day. It is also notable that the geomagnetic Kp and DST indices have no exhibited significant variations and differences on this day, indicating rather quiet geomagnetic condition.

Taking the GRACE-A and JASON-2 satellites, for example, Fig. 14 displays the scatter distribution of LEO-based plasmasphere VTEC values on DOY 183 in 2016 using GRACE-A and JASON-2 satellites data, considering the latitudes of GRACE-A and JASON-2 orbits as the x-axis. The LEO satellite can revolve the earth more than ten times in one day, thus there is more overlap in scatter distribution. The GRACE satellites are the polar-orbiting satellites with an orbital inclination of about 90°, while the JASON satellites have an orbital inclination of 66°. Thus, in Fig. 14, onboard observations of GRACE-A satellite cover the -90° to 90° of latitude space, and observation data of the JASON-2 satellite only occupy -66° to 66° of latitude space. The plasmasphere VTEC values using GRACE-A data by introducing GRACE-based VTEC model are within 27 TECU, while the VTEC results based on JASON-2 data and JASON VTEC model are about within 10 TECU. The LEO-based VTEC values are modeled into spherical harmonic function. Thus, VTEC results obtained from this method have the higher temporal and spatial resolution, which may cause slightly great variation ranges for GRACE-based VTEC results. Moreover, in 2016, before the expiration of satellite life, the highest and

lowest orbit heights of GRACE satellites have reduced to 392 and 355 km, respectively, which may contribute to some increment of VTEC results. The scatter distribution in Fig. 14 presents that the corresponding latitudes for GRACE-A-data-based VTEC peaks are located at about 0°–20° of north latitude, and the latitudes of JASON-2-data-based VTEC peaks are located at around 0°. In addition, we find that the JASON-2-data-based VTEC values have some negative values, and it is similar to the VTEC estimation results using ground station data. And this case also appears in the results of Wautelet et al. (2017) and Li et al. (2017a), and they reckon that DCBs parameters are underestimated. At present, there is no study to deal with the problem of negative values in LEO-based VTEC results. The reason of negative values may be the high height of JASON satellites and smaller absolute values of JASON-based plasmasphere VTEC. Another reason may be related to uneven data distribution. Due to uneven coverage of puncture point observations related to orbital inclination of 66° for JASON-2 satellite, it may lead to appear the negative values of VTEC. And this situation almost does not exist for GRACE satellites due to whole even coverage of observation data. According to statistics, when JASON-based VTEC results are non-negative, corresponding observation data of JASON-2 satellite can also cover -66° to 66° of latitude space (corresponding to orbit inclination of 66° for JASON satellites), and it doesn't affect final DCB estimation results. In Fig. 14, we show the non-negative VTEC results based on JASON-2 satellite orbits since the negative values have no physical meaning. The treatment of negative values in JASON-based VTEC is a problem that needs to be further studied. In addition, it is worth noting that if we would like to obtain the global LEO-based topside ionosphere, we should use the full coverage and even distributed LEO onboard data derived from polar-orbiting satellites with an orbital inclination of about 90°.

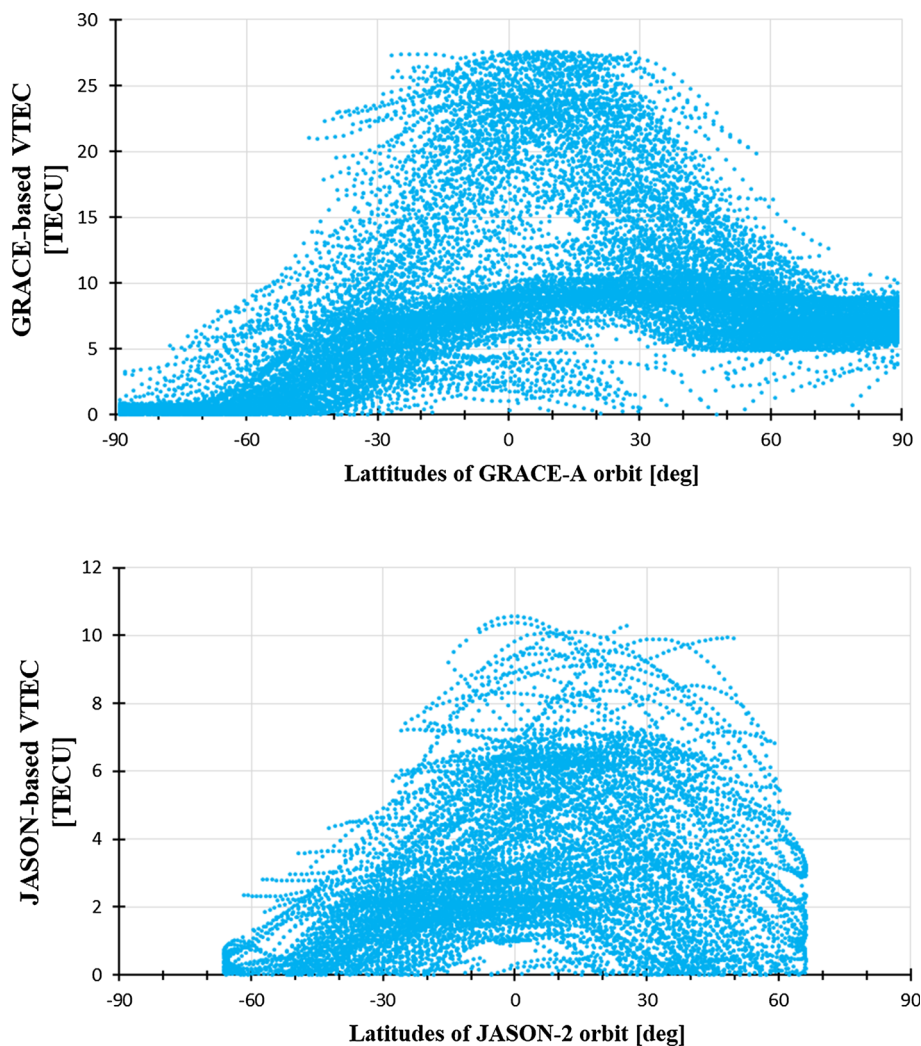
Fig. 13 Variations of solar and geomagnetic indices for July 2016: (top) solar radio flux at 10.7 cm; (middle) planetary K value (Kp indices); (bottom) disturbance storm time index (DST)



Mean (top) and STD (bottom) for the differences between the sum TEC, for LEO-based VTEC and IRI model, and the CODE GIM, during July 2016, are depicted in Fig. 15. During DCB estimation for multi-LEO data from different orbit heights, two LEO-based VTEC models were introduced—GRACE-based VTEC model and JASON-based VTEC model, which the GRACE-based VTEC model derived from the GRACE-A and -B satellites data, and the JASON-based VTEC model come from the JASON-2 and -3 satellites data. Since negative values have no physical meaning, we consider the negative values in JASON-based VTEC as 0. The mean of the difference between the sum TEC (the GRACE-based VTEC and IRI TEC) and the CODE GIM fluctuate around 4 TECU; the corresponding mean of difference between the sum TEC, for the JASON-based VTEC and IRI TEC, and the CODE GIM, are close 0 TECU approximately, with the range of -2 to 2 TECU. It can be seen, at the bottom of Fig. 15, that the STD values for the differences between the sum TEC, for the JASON-based VTEC and IRI TEC, and the CODE GIM fluctuate around 3 TECU

approximately, while the STDs for the GRACE-related differences fluctuate around 4 TECU. These statistics indicate that the differences between this sum TEC (GRACE-based VTEC plus IRI TEC) and the CODE GIM, are approximately 3.8 ± 3.8 TECU, while the JASON-related differences are approximately -0.2 ± 3.0 TECU. Considering that the altitude of GRACE satellites is less than 400 km, it is more complex for corresponding plasmasphere TEC compared with JASON satellites, with large absolute value and relatively low accuracy, while the corresponding plasmasphere TEC for the JASON satellites at the altitude of 1350 km is less complex than that obtained for the GRACE satellites, with the high accuracy. These comparisons indicate that the LEO-based VTEC exhibits relatively reliable results. The evaluation and accurate measurement for LEO-based VTEC are still a problem that needs further research. The next research work will aim to make the better reliability analysis of TEC provided by IRI model and obtain more reliable external TEC reference values for comparison analysis.

Fig. 14 LEO-based VTEC values scatter distribution based on GRACE-A and JASON-2 data, taking the latitudes of GRACE-A and JASON-2 orbits as the x-axis, respectively



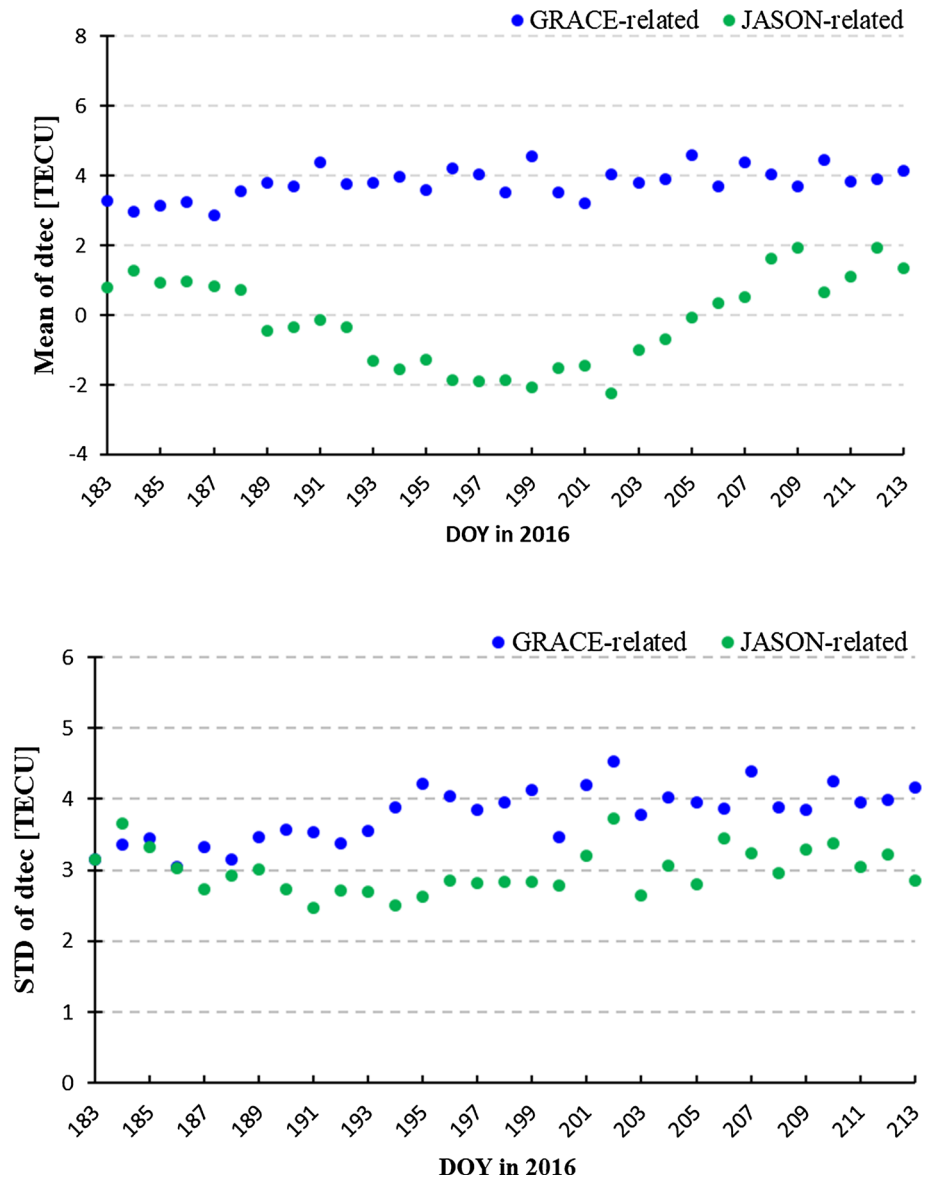
4 Conclusions

GPS satellite DCBs can be estimated using LEO data as a different method or as an alternate data source of ground stations. In this study, we simultaneously estimate GPS satellite DCBs, receiver DCBs, and LEO-based plasmasphere delay parameters using four LEO satellites from two different orbit heights. We proposed an ionosphere processing method for multi-LEO data from different orbit heights, which work by introducing the LEO-based VTEC models in advance to remove its effects. The two introduced VTEC models are derived from the modeling results using two paired LEO data from the same orbital height, respectively. Some conclusions have been drawn:

- (1) For GPS satellite DCB estimation using LEO data, the LEO-based VTEC is the main factor to influence DCBs estimation. It is also apparent that the more LEO data there are, the more stable the estimation results are, regardless of whether the onboard data are derived

from the same or different orbit heights. For LEO data from different orbit heights, we proposed to remove the plasmasphere delay effects in advance, by introducing the LEO-based VTEC models. It is worth noting that DCB estimation stability and accuracy can reach the superior results when multi-LEOs onboard data from different orbit heights are used. The mean difference and their standard deviations of GPS DCBs using multi-LEOs solution from different orbit heights relative to CODE products are better than those of single LEO and paired LEO solutions. The estimated GPS satellite DCBs accuracies RMS using multi-LEOs data from different heights are superior to that LEO schemes from either the same orbit height or single LEO schemes. Compared with the results of single LEO solutions, the monthly stabilities and accuracies for schemes GRACE-A and JASON-2 (two LEOs), the GRACE-A and -B and JASON-2 (three LEOs), and four LEOs from different orbit heights are improved by 25–35%, approximately.

Fig. 15 Mean (top) and STD (bottom) for differences between the summed TEC of the LEO-based VTEC and IRI 2016 and the CODE GIM, during July 2016. The blue points represent the related results of differences for the summed TEC (based on GRACE-A and -B plasmasphere VTEC and IRI model) with respect to CODE GIM; the green points represent the related results of differences for the summed TEC (based on JASON-2 and -3 plasmasphere VTEC and IRI model) with respect to CODE GIM



- (2) Using different LEO satellites from different orbit heights, the receiver DCB stability obtained using the same type of LEO satellites data at the same orbit heights are almost identical during the joint estimation, with the receiver DCB STDs based on GRACE series and JASON series satellites are 0.135 and 0.197 ns, respectively. The reasons may be that the paired LEO satellites have the same type receivers, and similar ionosphere activity characteristics due to similar satellite tracks that the paired receivers experienced.
- (3) To validate the realness of estimated LEO-based plasmasphere VTEC models, we compare the sum TEC of the LEO-based VTEC and IRI TEC, with the CODE GIM. The results indicate that the differences between the sum TEC (GRACE-based VTEC plus IRI TEC) and the CODE GIM are 3.8 ± 3.8 TECU; simi-

larly, the JASON-related differences are approximately -0.2 ± 3.0 TECU. These comparisons demonstrate that the LEO-based VTEC represent relatively reliable results.

DCB estimation stability and accuracy can reach the superior results when multi-LEOs onboard data from different orbit heights are used. Among all the schemes, the superior stability derived from simultaneous estimation using four LEO data at different orbit heights is 0.064 ns; the optimal accuracy for DCB estimation for different GPS satellites is the scheme GRACE-A and JASON-2 of 0.146 ns. Therefore, the stability and accuracy of LEO-based DCB estimations are similar to the level of ground station-based solutions. In order to improve the accuracy of GNSS DCB products further, we recommend using more LEOs data from the same

orbit heights to refine the LEO-based plasmasphere VTEC models and further optimize the error processing for DCB estimation. For example, the GPS group delay variations (GDV) may affect the stability of DCB estimation (Wanninger et al. 2017), which deserves further study as our next key research work. Moreover, the evaluation and accurate measurement for LEO-based VTEC are still a problem that needs further research, including making the better reliability analysis of TEC provided by IRI model and obtaining more reliable external TEC reference values for comparison analysis. In addition, according to the accuracy performance of estimation results using multi-LEO satellites data, it is also an effective method to consider weighting processing in DCB estimation. In this way, more LEO satellite data obtained from different orbit heights can be used to enhance navigation satellite products accuracy, also called navigation enhancement of LEO satellite.

Acknowledgements This work was supported by the Collaborative Precision Positioning Project funded by the Ministry of Science and Technology of China (No. 2016YFB0501900) and China Natural Science Funds (Nos. 41674022, 41674020). The authors acknowledge LU JIAXI International team program supported by the K.C. Wong Education Foundation and CAS. The authors are grateful to CODE for providing the DCB precise products. We are also grateful to the IRI Working Group for providing the IRI-2016 model code in Fortran. Meanwhile, we would like to thank the anonymous reviewers for their valuable comments.

Author contributions In this work, Y.Y. and M.L. proposed the idea and designed experiments; M.L. performed the research and wrote the initial draft; Y.Y. and X.H. revised the manuscript; M.L. and Y.C. provided research helps.

Data availability CODE's DCB products can be found at <ftp.aiub.unibe.ch/CODE/>. The onboard observation data for JASON and GRACE satellites are available at <ftp://avisoftp.cnes.fr/AVISO/pub/> and <ftp://isdftp.gfz-potsdam.de/>. The IRI-2016 model code in Fortran comes from the IRI homepage at irimodel.org.

Compliance with ethical standards

Conflict of interest The authors declare that they have no conflict of interest.

References

Bilitza D (2009) Evaluation of the IRI-2007 model options for the topside electron density. *Adv Space Res* 44:701–706

Bilitza D, Altadill D, Truhlik V, Shubin I, Galkin I, Reinisch B, Huang X (2017) International Reference Ionosphere 2016: from ionospheric climate to real-time weather predictions. *Space Weather* 15(2):418–429

Cerri L, BERTHIAS JP, Bertiger WI, Haines BJ, Lemoine FG, Mercier F, Ries JC, Willis P, Zelensky NP, Ziebart M (2010) Precision orbit determination standards for the Jason series of altimeter missions. *Mar Geod* 33:379–418

Foelsche U, Kirchengast G (2002) A simple “geometric” mapping function for the hydrostatic delay at radio frequencies and assessment of its performance. *Geophys Res Lett*. 29(10):111–1–111–4

Hernández-Pajares M, Juan JM, Sanz J, Aragón-Ángel A, García-Rigo A, Salazar D, Escudero M (2011) The ionosphere: effects, GPS modeling and the benefits for space geodetic techniques. *J Geod* 85(12):887–907

Hernández-Pajares M, Roma-Dollase D, Krankowski A, García-Rigo A, Orús-Pérez R (2017) Methodology and consistency of slant and vertical assessments for ionospheric electron content models. *J Geod* 91(12):1405–1414. <https://doi.org/10.1007/s00190-017-1032-z>

Kang Z, Tapley B, Bettadpur S, Ries J, Nagel P, Pastor R (2006) Precise orbit determination for the GRACE mission using only GPS data. *J Geod* 80:322–331

Krankowski A, Shagimuratov II, Ephishov II, Krypiak-Gregorczyk A, Yakimova G (2009) The occurrence of the mid-latitude ionospheric trough in GPS-TEC measurements. *Adv Space Res* 43(11):1721–1731

Li Z, Yuan Y, Li H, Ou J, Huo X (2012) Two-step method for the determination of the differential code biases of COMPASS satellites. *J Geod* 86(11):1059–1076

Li W, Li M, Shi C, Fang R, Zhao Q, Meng X, Bai W (2017a) GPS and BeiDou differential code bias estimation using Fengyun-3C satellite onboard GNSS observations. *Remote Sens* 9(12):1239. <https://doi.org/10.3390/rs9121239>

Li Z, Wang N, Li M, Zhou K, Yuan Y, Yuan H (2017b) Evaluation and analysis of the global ionospheric TEC map in the frame of international GNSS services. *Chin J Geophys* 60(10):3718–3729. <https://doi.org/10.6038/cjg20171003> (in Chinese)

Li X, Ma T, Xie W, Zhang K, Huang J, Ren X (2019) FY-3D and FY-3C onboard observations for differential code biases estimation. *GPS Solut*. <https://doi.org/10.1007/s10291-019-0850-2>

Lin J, Yue X, Zhao S (2014) Estimation and analysis of GPS satellite DCB based on LEO observations. *GPS Solut* 20(2):251–258. <https://doi.org/10.1007/s10291-014-0433-1>

Liu M, Yuan Y, Ou J, Chai Y (2019) Research on attitude models and antenna phase center correction for Jason-3 satellite orbit determination. *Sensors*. <https://doi.org/10.3390/s19102408>

Montenbruck O, Hauschild A (2013) Code biases in multi-GNSS point positioning. In: Proceedings of ION ITM 2013, San Diego

Montenbruck O, Hauschild A, Steigenberger P (2014) Differential code bias estimation using multi-GNSS observations and global ionosphere maps. *Navigation* 61(3):191–201. <https://doi.org/10.1002/navi.64>

Sanz J, Miguel-Juan J, Rovira-García A, González-Casado G (2017) GPS differential code biases determination: methodology and analysis. *GPS Solut* 21(4):1549–1561. <https://doi.org/10.1007/s10291-017-0634-5>

Schaer S (1997) How to use CODE's global ionosphere maps. University of Berne, Switzerland

Schaer S (1999) Mapping and predicting the earth's ionosphere using the global positioning system. Ph.D. Dissertation, University of Berne, Switzerland

Schaer S (2012) Activities of IGS Bias and Calibration Working Group. In: Meindl M, Dach R, Jean Y (eds) IGS Technical Report 2011. Astronomical Institute, University of Bern, Bern, pp 139–154

Wang N, Yuan Y, Li Z, Montenbruck O, Tan B (2015) Determination of differential code biases with multi-GNSS observations. *J Geod* 90(3):209–228. <https://doi.org/10.1007/s00190-015-0867-4>

Wanninger L, Sumaya H, Beer S (2017) Group delay variations of GPS transmitting and receiving antennas. *J Geod* 91(6):1–18

Wautelet G, Loyer S, Mercier F, Perosanz F (2017) Computation of GPS P1–P2 differential code biases with JASON-2. *GPS Solut* 21(4):1619–1631. <https://doi.org/10.1007/s10291-017-0638-1>

Xu G (2003) GPS theory, algorithms and applications. Springer, Berlin

- Yang Y, Mao Y, Sun B (2020) Basic performance and future developments of BeiDou global navigation satellite system. *Satell Navig* 1(1):1. <https://doi.org/10.1186/s43020-019-0006-0>
- Yuan Y (2002) Study on theories and method of correcting ionospheric delay and monitoring ionosphere based on GPS. Ph.D. Institute of Geodesy and Geophysics Chinese Academy of Sciences, Wuhan
- Yuan Y, Huo X, Zhang B (2017) Research progress of precise model and correction for GNSS ionospheric delay in china over recent years. *Acta Geod Cartogr Sin* 46(10):1364–1378
- Yuan Y, Wang N, Li Z, Huo X (2019) The Beidou global broadcast ionospheric delay correction model (BDGIM) and its preliminary performance evaluation results. *Navigation* 66(1):55–69. <https://doi.org/10.1002/navi.292>
- Yue X, Schreiner WS, Hunt DC, Rocken C, Kuo YH (2011) Quantitative evaluation of the low Earth orbit satellite based slant total electron content determination. *Space Weather*. <https://doi.org/10.1029/2011sw000687>
- Zakharenkova I, Cherniak I (2015) How can GOCE and TerraSAR-X contribute to the topside ionosphere and plasmasphere research? *Space Weather* 13(5):271–285
- Zhang X, Ma F (2019) Review of the development of LEO navigation-augmented GNSS. *Acta Geod Cartogr Sin* 48(9):1073–1087. <https://doi.org/10.11947/j.AGCS.2019.20190176>
- Zhang X, Tang L (2014) Estimation of COSMIC LEO satellite GPS receiver differential code bias. *Chin J Geophys* 57(2):377–383 (in Chinese)
- Zhang B, Ou J, Yuan Y, Li Z (2012) Extraction of line-of-sight ionospheric observables from GPS data using precise point positioning. *Sci China Earth Sci* 55(11):1919–1928
- Zhong J, Lei J, Dou X, Yue X (2015a) Assessment of vertical TEC mapping functions for space-based GNSS observations. *GPS Solut* 20(3):353–362. <https://doi.org/10.1007/s10291-015-0444-6>
- Zhong J, Lei J, Dou X, Yue X (2015b) Is the long-term variation of the estimated GPS differential code biases associated with ionospheric variability? *GPS Solut* 20(3):313–319. <https://doi.org/10.1007/s10291-015-0437-5>
- Zhong J, Lei J, Yue X, Dou X (2016) Determination of differential code bias of GNSS receiver onboard low earth orbit satellite. *IEEE Trans Geosci Remote Sens* 54:4896–4905. <https://doi.org/10.1109/TGRS.2016.2552542>
- Zhou P, Nie Z, Xiang Y, Wang J, Du L, Gao Y (2019) Differential code bias estimation based on uncombined PPP with LEO onboard GPS observations. *Space Res, Adv*. <https://doi.org/10.1016/j.asr.2019.10.005>